

# Weak-value-amplification analysis beyond the AAV limit of weak measurements

Jianhua Ren, Lupei Qin, Wei Feng, and Xin-Qi Li\*

Center for Joint Quantum Studies and Department of Physics, School of Science,  
Tianjin University, Tianjin 300072, China

(Dated: April 3, 2020)

The weak-value (WV) measurement proposed by Aharonov, Albert and Vaidman (AAV) has attracted a great deal of interest in connection with quantum metrology. In this work, we extend the analysis beyond the AAV limit and obtain a few main results. (i) We obtain non-perturbative result for the signal-to-noise ratio (SNR). In contrast to the AAV's prediction, we find that the SNR asymptotically gets worse when the AAV's WV  $A_w$  becomes large, i.e., in the case  $g|A_w|^2 \gg 1$ , where  $g$  is the measurement strength. (ii) With the increase of  $g$  (but also small), we find that the SNR is comparable to the result under the AAV limit, while both can reach – actually the former can slightly exceed – the SNR of the standard measurement. However, along a further increase of  $g$ , the WV technique will become less efficient than the standard measurement, despite that the postselection probability is increased. (iii) We find that the Fisher information can characterize the estimate precision qualitatively well as the SNR, yet their difference will become more prominent with the increase of  $g$ . (iv) We carry out analytic expressions of the SNR in the presence of technical noises and illustrate the particular advantage of the imaginary WV measurement. The non-perturbative result of the SNR manifests a favorable range of the noise strength and allows an optimal determination.

## I. INTRODUCTION

Quantum weak measurement with postselection was initially proposed by Aharonov, Albert, and Vaidman (AAV) in their seminal work [1, 2]. The marked feature of this type of measurement is that the resultant quantum weak values (WV) can exceed the range of eigenvalues of the observable. Despite the long time debate with theoretical curiosity, the concept of WV has been found useful in quantum metrology, e.g., in developing novel schemes of quantum state tomography [3–5] and for weak signal amplifications in parameter estimation [6–24], while the latter application has been termed as weak-value amplification (WVA) technique in literature.

As demonstrated in the early representative experiments, e.g., the first observation of the spin Hall effect of light [6] and measuring the small transverse deflections of an optical beam with extremely high resolution [7–10], the WVA technique can lead to an amplification phenomenon, just like a small image magnified by a microscope. The amplification effect is of great interest from the experimental perspective, since it gives access to an experimental sensitivity beyond the detector's resolution, making thus possible to measure very small physical effects. For the optical beam-deflection measurement, this technique also allows to use high power lasers with low power detectors while maintaining the optimal signal-to-noise ratio (SNR), and holds the ability to obtain the ultimate limit in deflection measurement with a large beam radius [7–10]. In regard to this similar advantage, it was also pointed out that the WVA technique can outperform conventional measurement in the presence of detector saturation [21]. Finally and importantly, the WVA technique can have remarkable advantages of reducing technical noise in some circumstances [6–8, 12, 15, 17, 18, 25–27].

On the other hand, theoretical understanding highlights that

the WVA technique can put all of the information about the detected parameter into a small portion of the events (after postselection) and claims that this fact alone gives technical advantages [25–27]. However, there existed controversial debates about the WVA advantage against technical noises, with diverse opinions and some negative comments [28–30]. It seems now clear that at least the scheme based on the imaginary WV measurement has sound potentials to outperform standard measurement in the presence of technical noise [12, 15, 26, 27], e.g., by several orders of magnitude [12].

We notice that so far the large number of investigations on the WVA merits analysis have been largely restricted in the treatment under the AAV limit. Despite that the generalized results of WV beyond the AAV limit have been developed in different contexts and with different forms [31–40], few efforts were found to combine these results with parameter estimations [25, 26]. In Ref. [25], analysis for frequency-shift measurement based on the Mach-Zehnder interferometer was presented in the absence of technical noise, with a particular treatment beyond the AAV limit and focusing on the quantum shot noise from the photon number fluctuations. Meanwhile, in Ref. [26], which presents a clear analysis for the imaginary WV measurement and how the technical noise can be used to enhance the SNR, numerical results beyond the AAV limit were carried out to show a reasonable behavior for the noise strength dependence, while the main theoretical (analytic) analysis was restricted in the AAV limit.

In this work, along the lines of Refs. [26, 27], which contain the typical analysis based on the SNR and Fisher information, we apply the WV treatment beyond the AAV limit to analyze the WVA measurement for parameter estimation. Our systematic generalizations are based on the quantum Bayesian approach (or its variant) for partial-collapse weak measurement [41–44], which allows us to update the system state efficiently from a specific readout of the meter's variable. Then, the subsequent postselection of the system state allows us to construct a *joint probability* distribution by means of the chain-rule in probability theory, which also enables us to account

---

\*Electronic address: xinqi.li@tju.edu.cn

for the various technical noises very straightforwardly. Using the joint probability we are able to carry out, conveniently and analytically, the expectation and variance of the postselected measurement results of the meter's variable, for the use of the SNR characterization.

The paper is organized as follows. In Sec. II we carry out the generalization in terms of the SNR characterization, with the results beyond the AAV limit in close parallel to the compact forms under the AAV treatment. In Sec. III we continue the generalization by computing the Fisher information, also along the lines of analysis under the AAV limit. Analogy and difference between the SNR and Fisher information characterizations will be displayed in connection with the generalized treatment for finite measurement strength, via examination of the Cramér-Rao bound. We further complete the generalization in Sec. IV by including technical noise and in particular analyze the remarkable results of imaginary WVA measurements. In Sec. V we summarize the work with brief remarks.

## II. SIGNAL-TO-NOISE RATIO CHARACTERIZATION

### A. AAV's weak values

Let us recall briefly some basic aspects of the weak values (WV). In general, consider two coupled systems (or the degrees of freedom of a single system), described by the coupling Hamiltonian  $H' = \kappa AB$ , with  $\kappa$  the coupling strength,  $A$  the *system* operator, and  $B$  the operator of the *measuring device* (meter). The weak value  $A_w$ , defined by a pair of preselected and postselected (PPS) states of the system, manifests itself as the meter's *shift* in the wave function of the measuring device.

To be more specific, following the AAV's original treatment, let us take the Stern-Gerlach setup as a concrete model, which is equivalent in theory to many other systems in lab, such as the optical beam-deflection measurements in quantum optics and the circuit-QED architecture in solid-state quantum computation. In the Stern-Gerlach setup, the electron's trajectory is deflected when it passing through the inhomogeneous magnetic field. In this context, we treat the spin degree of freedom of the electron as the *system* and the spatial one (coordinate or momentum) as the *meter*, while their interaction is described by  $H' = \kappa PA$ , with  $P$  the momentum operator and  $A = \sigma_z$  the Pauli operator for the spin. We assume that the system and the meter are initially prepared as  $|\Psi_T\rangle = |i\rangle|\Phi\rangle$ , where the system state reads  $|i\rangle = \alpha|1\rangle + \beta|2\rangle$ , and the meter's state (the transverse wavefunction of the electron) is assumed as a Gaussian,  $\Phi(x) = (2\pi\sigma^2)^{-1/4} \exp[-x^2/(4\sigma^2)]$ , with  $\sigma$  the width of the wavepacket. Associated with the coupling Hamiltonian, the evolution of the entire state is governed by the unitary operator  $U = e^{-idPA}$ , with  $d = \int_0^\tau dt \kappa = \kappa\tau$  ( $\tau$  is the interacting time). After the interaction, the entire state becomes entangled and is given by

$$|\tilde{\Psi}_T\rangle = \alpha|1\rangle|\Phi_1\rangle + \beta|2\rangle|\Phi_2\rangle, \quad (1)$$

where the meter's wavefunctions read

$$\Phi_j(x) = \frac{1}{(2\pi\sigma^2)^{1/4}} \exp\left[-\frac{(x - \bar{x}_j)^2}{4\sigma^2}\right]. \quad (2)$$

with  $\bar{x}_{1,2} = \pm d$  the Gaussian centers shifted by the system states  $|1\rangle$  and  $|2\rangle$ , respectively.

Under the AAV limit (weak enough measurement), it can be proved that after postselection with  $|f\rangle$  for the system state, the meter's wavefunction is approximately given by [1, 2]

$$\tilde{\Phi}(x) = \frac{1}{(2\pi\sigma^2)^{1/4}} \exp\left[-\frac{(x - A_w d)^2}{4\sigma^2}\right], \quad (3)$$

where the multiplicative factor reads

$$A_w = \frac{\langle f|A|i\rangle}{\langle f|i\rangle}. \quad (4)$$

This is the well known weak values proposed by AAV. For the readout of  $x$ , its average associated with the new ensemble defined by  $|i\rangle$  and  $|f\rangle$  (the PPS states) is given by  ${}_f\langle x \rangle_i = (\text{Re}A_w) d$ . Since  $A_w$  can be very large (strongly violating the bounds of the eigenvalues of  $A$ ), we say then that the signal is *amplified*, with the amplification factor defined by

$$\eta = |{}_f\langle x \rangle_i| / d. \quad (5)$$

In the latter part of this work, we will use  $\eta$  as well to denote the amplification rate for finite strength of measurements, going beyond the AAV limit. Finally, we may briefly mention that the AAV's WV is a result of postselection, with the postselection probability

$$\gamma = |\langle f|i\rangle|^2. \quad (6)$$

Through the whole work, we will also use  $\gamma$  to denote the postselection probability under finite strength measurements.

### B. Analysis under the AAV limit

As mentioned above, with the postselection involved measurement, the signal of the parameter is amplified as  $\tilde{d} = (\text{Re}A_w)d$ , which can be much larger than the original  $d$ . From the noisy quantum measurement, both parameters  $d$  and  $\tilde{d}$  'hide' in the distribution functions, say, the original distribution  $P(x|d) = |\Phi_1(x)|^2$  and the postselected one  $\tilde{P}(x|\tilde{d}) = |\tilde{\Phi}(x)|^2$ . Below, we analyze the estimate precision associated with this weak-value-amplification (WVA) technique. (i) If we use only *one output data* for the estimation of the parameter for each of both cases, the imprecision is characterized by the statistical variance of the distribution function. This is the so-called quantum shot noise. For instance, for  $d$ , the imprecision of estimate is characterized by  $\delta^2(\hat{d}) = \overline{x^2} - (\overline{x})^2 = \sigma^2$ , where  $\overline{(\dots)}$  means the average defined by the distribution function  $P(x|d)$ . Similar characterization applies as well for  $\tilde{d}$ , with  $\delta^2(\tilde{\hat{d}}) \equiv \tilde{\sigma}^2 = \sigma^2$ , based on the result of Eq. (3). (ii) If we use  $N$  measurement data, i.e., using  $\hat{d} = \frac{1}{N} \sum_{j=1}^N x_j$

as the estimator, the estimate precision will be improved as  $\delta^2(\hat{d}) = \sigma^2/N$ . For the WVA technique, let us suppose  $N'$  data survived from the  $N$  outputs by postselection, and use  $\tilde{d} = \frac{1}{N'} \sum_{j=1}^{N'} x_j$  as the estimator. The estimate precision for  $\tilde{d}$  is characterized by the variance  $\delta^2(\tilde{d}) = \sigma^2/N'$ .

Therefore, as the most direct characterization for the estimate precision, we follow Ref. [26] to introduce the signal-to-noise ratio (SNR) as

$$R_{S/N}^{(w)} = \frac{\tilde{d}}{\sigma/\sqrt{N'}} = \sqrt{\gamma}\eta R_{S/N}^{(s)}, \quad (7)$$

where  $R_{S/N}^{(s)} = \frac{d}{\sigma/\sqrt{N}}$  is the SNR of the standard method,  $\gamma = N'/N$  the success probability of postselection, and  $\eta = \tilde{d}/d$  the amplification rate of the signal. Under the AAV limit, we find  $\sqrt{\gamma}\eta = |\langle f|A|i\rangle| = |A_{fi}|$ , which can approach unity by a proper choice of the PPS states. For instance, consider  $A = \sigma_z$  and choose  $|i\rangle = |\uparrow\rangle_x$  and  $|f\rangle \simeq |\downarrow\rangle_x$  (the eigenstates of  $\sigma_x$ ). Here we map the two-states system to a spin-1/2 particle described by the Pauli operators, with the correspondence of  $|1\rangle = |\uparrow\rangle_z$  and  $|2\rangle = |\downarrow\rangle_z$ . Under such choice for the PPS states, we see that the SNRs of both schemes are almost the same.

In this context, an interesting comment follows that in the WVA scheme the postselection keeps only a sub-ensemble of the measurement data, however it can reach similar estimate precision. In addition to the technical advantages in practice [6–10, 21], this feature alone is rather unusual, especially from the perspective of the Fisher information [27]. That is, the postselection makes the sub-ensemble of data contain roughly the same amount of information of the whole ensemble of data.

### C. Results beyond the AAV limit

In order to extend the AAV's treatment to finite strength measurement, a key element is to update the initial (preselected) state  $\rho_i = |i\rangle\langle i|$  based on the measurement result  $x$ . This can be done by applying the quantum Bayesian approach [41–44], or directly using Eq. (1) for the present case. Conditioned on  $x$ , we formally denote the update as  $\rho_i \rightarrow \tilde{\rho}(x)$ . Accordingly, the  $x$  associated postselection probability is simply given by  $P_x(f) = \langle f|\tilde{\rho}(x)|f\rangle$ . Based on this, neglecting  $x$  (summing all the  $x$  which passed the postselection), we obtain the total postselection probability as [38–40]

$$\begin{aligned} \gamma &= \int dx P_i(x) P_x(f) \\ &= \rho_{f11}\rho_{i11} + \rho_{f22}\rho_{i22} \\ &\quad + 2 \operatorname{Re}(\rho_{f12}^* \rho_{i12}) e^{-(\bar{x}_1 - \bar{x}_2)^2/8\sigma^2}, \end{aligned} \quad (8)$$

which is a generalization of the AAV result,  $\gamma = |\langle f|i\rangle|^2$ . In deriving this result, we have used  $P_i(x) = \rho_{i11}|\Phi_1(x)|^2 + \rho_{i22}|\Phi_2(x)|^2$ , and  $\rho_f = |f\rangle\langle f|$  for the postselection state.

Actually, it is desirable to introduce the *joint* probability of getting  $x$  and passing the postselection of  $|f\rangle$

$$\Pr(f; x) = P_i(x) P_x(f) / \mathcal{N}, \quad (9)$$

while the normalization factor  $\mathcal{N}$  is just equal to  $\gamma$ . Using  $\Pr(f; x)$ , ensemble averages of  $x$  and  $x^2$  can be easily calculated. First, let us consider the average of  $x$ , i.e.,  $f\langle x\rangle_i = \int dx x \Pr(f; x)$ , from which the amplification rate of the parameter is simply given by  $\eta = |f\langle x\rangle_i|/d$ . After some algebras, we obtain [38–40]

$$\frac{f\langle x\rangle_i}{d} = \frac{\operatorname{Re}A_w}{1 + \mathcal{G}(|A_w|^2 - 1)} \equiv \frac{\operatorname{Re}A_w}{\mathcal{M}}. \quad (10)$$

Here we introduced  $\mathcal{G} = (1 - e^{-2g})/2$  and  $g = (d/2\sigma)^2$ , which is a suitable parameter to characterize the measurement strength. We also defined the *modification* factor  $\mathcal{M}$ , which clearly reflects the modification effect to the AAV result. In the limit of *extremely weak* measurement, we have  $\mathcal{G} = g \rightarrow 0$ . Then, it seems that we can make the limiting  $\mathcal{M} \rightarrow 1$  and return to the AAV result. However, this is true only for the case that the AAV weak value  $A_w$  is not large enough. In the regime of the *anomalous* AAV effect, i.e., when  $A_w \rightarrow \infty$ , the  $\mathcal{M}$  factor might be large and will seriously modify the result, even in the 'extremely' weak measurement regime.

Under the AAV limit, the distribution of the postselected  $x$  is still a Gaussian, with a shifted center but the same width  $\sigma$ , as shown by Eq. (3). Now, for finite strength measurement, the distribution  $\Pr(f; x)$  is no longer a Gaussian in general, and may have a different width  $\tilde{\sigma}$ . We therefore calculate  $f\langle x^2\rangle_i$ , using the distribution function  $\Pr(f; x)$ . After some algebras, we obtain

$$\begin{aligned} \tilde{\sigma}^2 &= f\langle x^2\rangle_i - (f\langle x\rangle_i)^2 \\ &= \sigma^2 + d^2\eta \left( \frac{|A_w|^2 + 1}{2\operatorname{Re}A_w} - \eta \right). \end{aligned} \quad (11)$$

For the convenience of later use, we further introduce a *width change factor* as

$$\eta_\sigma = \frac{\tilde{\sigma}}{\sigma} = \left[ 1 + 4g\eta \left( \frac{|A_w|^2 + 1}{2\operatorname{Re}A_w} - \eta \right) \right]^{1/2}. \quad (12)$$

Precisely in parallel to Eq. (7) under the AAV limit, we introduce the SNR for the weak value measurement with finite strength,  $R_{S/N}^{(w)} = \tilde{d}/(\tilde{\sigma}/\sqrt{N'})$ , where  $\tilde{d} = |f\langle x\rangle_i|$  is given by Eq. (10). We further rescale it as

$$\begin{aligned} R_{S/N}^{(w)} &= \left( \frac{d}{\sigma/\sqrt{N}} \right) (\sqrt{\gamma}\eta/\eta_\sigma) \\ &\equiv R_{S/N}^{(s)} (\sqrt{\gamma}\eta/\eta_\sigma), \end{aligned} \quad (13)$$

where  $R_{S/N}^{(s)}$  is the SNR of the standard measurement. By this way, the SNR comparison of the two measurement schemes is fully captured by the factor

$$\mathcal{R} = \sqrt{\gamma}\eta/\eta_\sigma. \quad (14)$$

In Fig. 1, we analyze this factor in detail by numerical plots of the key variables associated with it.

In Fig. 1(a), we show the postselection probability. In the weak value related application problems, the most interesting regime is that by setting the postselection state  $|f\rangle$  nearly orthogonal to the initial state  $|i\rangle$ . This will result in *anomalous* weak values. However, with the increase of the measurement strength, the initial state  $|i\rangle$  will be disturbed more seriously by the measurement backaction. This makes the disturbed state no longer nearly orthogonal to the initial state  $|i\rangle$ , causing thus an increase of the postselection probability with the measurement strength, as shown in Fig. 1(a).

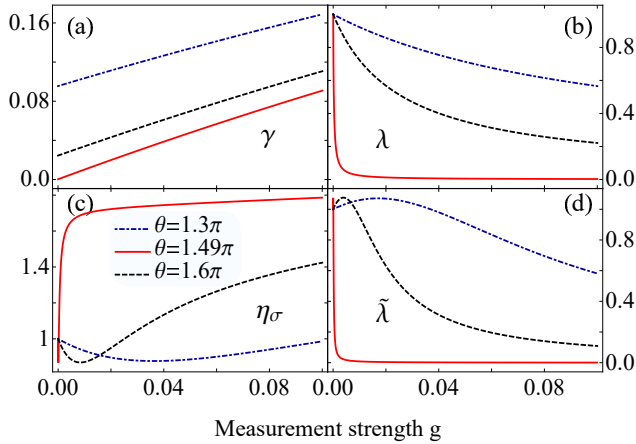


FIG. 1: Numerical plots as a function of the measurement strength  $g$ , for the a few variables in the SNR scaling factor,  $\mathcal{R} = \sqrt{\gamma}\eta/\eta_\sigma$ , given by Eq. (14). In (a) and (b), we show the postselection probability  $\gamma$  and the  $\lambda$  factor which is defined by  $\lambda = \gamma\eta^2/|A_{fi}|^2$ , where  $\eta$  is the amplification rate of the signal and the trivial factor  $A_{fi} = \langle f|A|i\rangle$  is scaled out for a reason as explained in the main text. In (c) we plot the width change factor  $\eta_\sigma = \tilde{\sigma}/\sigma$ , then in (d) we further include its effect into the scaling factor of the SNR by introducing  $\tilde{\lambda} = \lambda/\eta_\sigma^2$ . All the plots are exemplified by the PPS states  $|i\rangle = (|1\rangle + |2\rangle)/\sqrt{2}$  and  $|f\rangle = \cos(\frac{\theta}{2})|1\rangle + \sin(\frac{\theta}{2})|2\rangle$ , with  $\theta = 1.3\pi$ ,  $1.49\pi$  and  $1.6\pi$ , respectively.

In the WVA problem, the role of the post-selection is twofold: it holds the advantage of getting an amplified signal, while at the same time it suffers the disadvantage of discarding data, then with a small post-selection probability. The two competing elements of this type are well described by  $\gamma$  and  $\eta$ . Under the AAV limit, we simply find  $\gamma\eta^2 = |\langle f|A|i\rangle|^2$ , while the trivial factor  $A_{fi} = \langle f|A|i\rangle$  can approximately be unity by proper design of the initial and post-selection states. For finite strength measurement, it is not clear how these two factors compete to each other. We may thus consider the quantity  $\gamma\eta^2$  and in particular to scale out the trivial factor by introducing  $\lambda = \gamma\eta^2/|A_{fi}|^2$ . In the AAV limit, we simply have  $\lambda = 1$ .

In Fig. 1(b) we show the behavior of  $\lambda$  as a function of the measurement strength, for a couple of post-selection states. The common feature is that the factor  $\lambda$  decreases from unity (the limiting value as  $g \rightarrow 0$ ) with the increase of the measurement strength, which indicates a *gradual inefficiency* of the WVA technique. In particular, even for considerably weak measurement strengths, care is needed for the design of the

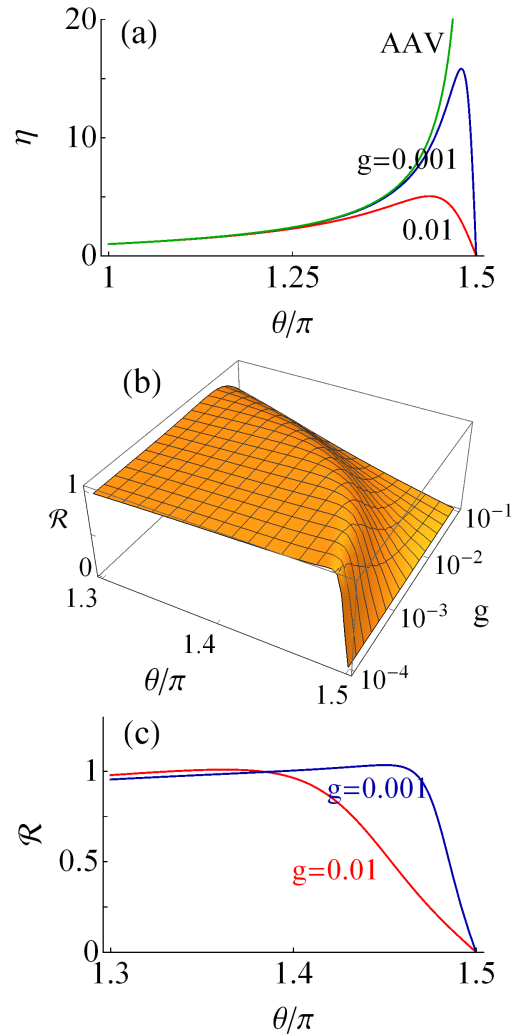


FIG. 2: (a) Deviation of the non-perturbative result, Eq. (10), from the AAV's prediction when  $A_w$  becomes large. (b) The overall result of the SNR (scaled by the result of conventional measurement), while the deviation effect in (a) is manifested here by the 'fall-down' area. (c) A more evident plot complementary to (b), using two measurement strengths. Notation of the PPS states  $|i\rangle$  and  $|f\rangle$  is the same as in Fig. 1.

pre- and post-selection states: one should not make the AAV weak value  $A_w$  too 'anomalous', roughly speaking, which should satisfy the condition  $g|A_w|^2 \ll 1$ . The result displayed by the red curve in Fig. 1(b) is an example of this effect, which indicates a failure of the WVA technique in this case, despite that the associated AAV weak value  $A_w$  is 'anomalously' large. We may remark that this effect cannot be revealed from the standard AAV result broadly employed in the WVA literature. Actually, this effect is a consequence of the more rigorous result of Eq. (10), caused by the denominator of the modification factor  $\mathcal{M}$ . We will return to this point again after a while, with the particular plot of Fig. 2.

As we have pointed out, beyond the AAV limit, the distribution of the postselected data from finite strength of measurement can considerably deviate from the Gaussian, and have a



different width as shown by Eq. (11). In Fig. 1(c) we plot the width change factor  $\eta_\sigma = \tilde{\sigma}/\sigma$ , which is given by Eq. (12), as a function of the measurement strength, while in Fig. 1(d) we further include this effect into the scaling factor  $\lambda$  of the SNR by introducing  $\tilde{\lambda} = \lambda/\eta_\sigma^2$ . We find that the modification effect is observable, especially showing a non-monotonic behavior with the maximum larger than unity. However, after accounting for the factor  $|A_{fi}|^2$ , as shown in Fig. 2, the signal-to-noise ratio of the WVA measurement is bounded (approximately) by the result of the standard measurement.

Let us continue the discussion related to the ‘red curve’ in Fig. 1(b). We know that if the PPS states  $|i\rangle$  and  $|f\rangle$  are nearly orthogonal, the *anomalous* weak value  $A_w$  can violently exceed the bounds of the eigenvalues of the operator  $A$ . For the WVA problem, the standard AAV treatment predicts that  $\text{Re}A_w$  (or  $\text{Im}A_w$ ) is the amplification rate of the signal. However, based on a non-perturbative treatment, the resultant Eq. (10) indicates that the amplification rate will strongly deviate from the AAV’s prediction when  $A_w$  becomes too ‘anomalously’ large. We clearly show this behavior by the plot of Fig. 2(a).

As a consequence of this behavior, we show in Fig. 2(b) the overall result of the SNR (scaled by the result of the standard measurement), after accounting for the effects of all the elements of  $\gamma$  (post-selection probability),  $\eta$  (signal amplification) and  $\eta_\sigma$  (change of distribution width). The ‘fall-down’ area (from unity to almost zero) is a direct consequence of the behavior mentioned above for Fig. 2(a). This ‘fall-down’ behavior indicates that, out of our simple expectation, not a larger  $A_w$  will necessarily result in a better effect of amplification. In practice, one should avoid this area by designing proper post-selection which, very trickily, depends on the measurement strength. After avoiding the ‘dangerous’ area, the results shown in Fig. 2(b) and in the complementary Fig. 2(c) display a flat regime with  $\mathcal{R} \simeq 1$ , i.e., reaching nearly the SNR of the standard method. Actually, in Fig. 2(c), we notice that the SNR can even slightly exceed the result of the standard measurement, while the result under the AAV limit is strictly bounded by the SNR of the conventional method [27]. Again, we emphasize that all the insights gained above are possible only from the non-perturbative treatment.

### III. FISHER INFORMATION CHARACTERIZATION

#### A. Concept of Fisher information

In general, for a parameter- $\Omega$  dependent probability distribution of a random variable  $x$ ,  $P(x|\Omega)$ , the Fisher information is defined as [45]

$$\mathcal{F}(\Omega) = \int dx P(x|\Omega) [\partial_\Omega \ln P(x|\Omega)]^2. \quad (15)$$

This is the available *information* about the unknown parameter  $\Omega$ , or a measure of the sensitivity of  $P(x|\Omega)$  to the parameter  $\Omega$ . Fisher information is additive. That is, for  $N$  independent trials, the total information is simply given by  $\mathcal{F}_N(\Omega) = N\mathcal{F}(\Omega)$ . So the most relevant quantity is the

Fisher information extracted by a single probe trial, given by Eq. (15). For parameter estimation, the estimator of  $\Omega$ , denoted as  $\hat{\Omega}$ , has the following properties: (i) its expectation value satisfies  $E(\hat{\Omega}) = \Omega$ ; (ii) its variance is bounded by the Cramér-Rao bound (CRB) as  $\delta^2(\hat{\Omega}) \geq 1/\mathcal{F}(\Omega)$ . This inequality shows that the Fisher information sets the minimal estimate uncertainty of  $\Omega$ .

As a little bit extension, if  $E(\hat{\Omega}) \neq \Omega$ , i.e., the expectation value of the estimator is connected to the *original* parameter via certain functional relation, the CRB inequality reads [45]

$$[\partial_\Omega E(\hat{\Omega})]^2 \leq \mathcal{F}(\Omega) \delta^2(\hat{\Omega}). \quad (16)$$

From this result we see that the Fisher information actually sets the upper bound of the SNR, by noting that  $\delta^2(\hat{\Omega})$  characterizes the extent of the shot noise of the quantum measurement, while  $\partial_\Omega E(\hat{\Omega})$  describes the amplification of the signal (the parameter). Applying the CRB inequality to the WVA problem, we may proceed with the following discussions and results.

#### B. Analysis under the AAV limit

Let us consider first the standard method. We identify  $\Omega = d$  and the estimator  $\hat{\Omega} = \hat{d}$ , which satisfies  $E(\hat{d}) = d$ . Substituting the Gaussian distribution Eq. (2) into the formula of the Fisher information Eq. (15), simple calculation yields  $\mathcal{F} = 1/\sigma^2$ . Compared with the estimate precision  $\delta^2(\hat{d}) = \sigma^2$ , we find that the CRB inequality is saturated as an equality,  $\delta^2(\hat{d}) = 1/\mathcal{F}$ .

Then, let us consider the WVA scheme. We identify  $\Omega = d$  and  $E(\hat{\Omega}) = E(\tilde{d}) = \eta d$ , with  $\eta = |\text{Re}A_w|$ . Under the AAV limit, the distribution function of the postselected data is still a Gaussian, which gives Fisher information as  $\tilde{\mathcal{F}} = \eta^2/\sigma^2$ . Again, this result saturates also the CRB inequality,  $\delta_w^2(\hat{d}) = 1/\tilde{\mathcal{F}}$ . Indeed, the Fisher information carried by each postselected data is enhanced by a factor  $\eta^2$ , compared to that without postselection.

As done in the SNR characterization, we further account for the effect of the postselection probability. For many runs of measurements using  $N$  particles, the total Fisher information of the  $N'$  post-selected particles read

$$\tilde{\mathcal{F}}_{N'} = N'\eta^2/\sigma^2 = \gamma\eta^2 \mathcal{F}_N, \quad (17)$$

where  $\mathcal{F}_N = N/\sigma^2$  is the total Fisher information of the  $N$  particles without postselection. Noting that under the AAV limit  $\gamma\eta^2 = |\langle f|A|i\rangle|^2$  (which can approach unity), we see then, precisely as the SNR discussed in Sec. II (B), that the post-selection makes the sub-ensemble of data ( $N'$  particles) encode roughly the same amount of Fisher information as the whole ensemble ( $N$  particles), quite surprisingly, by noting that  $N \gg N'$ .

### C. Results beyond the AAV limit

Going beyond the AAV limit, let us consider the case of weak measurement with finite strength. After postselection, the distribution of outputs is largely distorted from the simple Gaussian, i.e.,  $P_{f,i}(x) = P_i(x)P_x(f)/\mathcal{N}$ , with  $\mathcal{N}$  denoting the normalization factor. Since  $P_x(f)$  is  $x$  dependent in general, we know that the new distribution might deviate seriously from  $P_i(x)$ . In the above, this postselected distribution has been characterized by the expectation value and variance of  $x$ . Now we further employ the Fisher information to characterize the effect of postselection. Again, we identify  $\Omega = d$  and  $E(\hat{\Omega}) = E(\tilde{d}) = \eta d$ . Noting that  $\eta$  is of  $d$  dependence, we introduce  $\tilde{\eta} = \partial_d(\eta d) = \eta + (\partial_d \eta)d$ . We also denote the variance  $\delta^2(\tilde{d}) = \tilde{\sigma}^2$ . Then, from the CRB inequality we have

$$\tilde{\eta}^2/\eta_\sigma^2 \leq \tilde{\mathcal{F}}/\mathcal{F}. \quad (18)$$

Here we have used  $\eta_\sigma = \tilde{\sigma}/\sigma$  and  $\mathcal{F} = 1/\sigma^2$ .

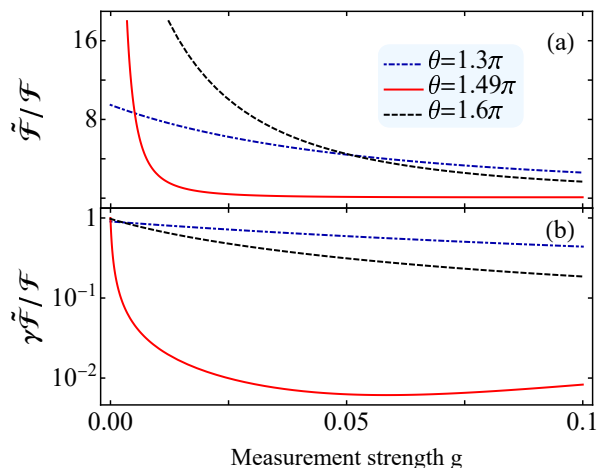


FIG. 3: (a) Enhancement of the Fisher information of a single trial, as a function of the measurement strength. (b) Tradeoff result of  $\gamma\tilde{\mathcal{F}}/\mathcal{F}$ , after accounting for the effect of the postselection probability. The PPS states are assumed the same as in Fig. 1.

In Fig. 3(a), we illustrate the enhancement of the Fisher information of a single trial, by numerically plotting  $\tilde{\mathcal{F}}/\mathcal{F}$  as a function of the measurement strength. The reason of the enhancement is also rooted in the new distribution of the postselected data, which are shifted/amplified by the postselection. In Ref. [27], this enhancement was highlighted by that each postselected data contains more Fisher information, i.e.,  $\tilde{\mathcal{F}}/\mathcal{F} \gg 1$ . However, after accounting for the effect of the postselection probability  $\gamma = N'/N$ , we find that the tradeoff result  $\gamma\tilde{\mathcal{F}}/\mathcal{F}$  cannot be larger than unity, for arbitrary measurement strength and post-selection, as shown in Fig. 3(b).

In Fig. 4, we further examine the CRB inequality (18) through numerical results. Under the AAV limit, one can check that Eq.(18) would reduce as an equality. However, for the more general case, we find here that the CRB inequality

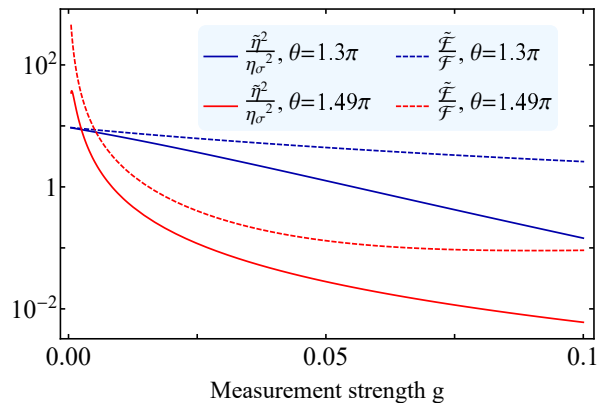


FIG. 4: Examination of the CRB inequality,  $\tilde{\eta}^2/\eta_\sigma^2 \leq \tilde{\mathcal{F}}/\mathcal{F}$ , which is found to be unsaturated with the increase of the measurement strength. The PPS states are assumed the same as in Fig. 1.

ity is becoming unsaturated with the increase of the measurement strength. This might be an interesting point in regard to the CRB inequality itself. The generic reason seems not very obvious, i.e., from the mathematical derivation of the CRB inequality. We may leave this issue for possible future investigations.

Roughly speaking, the left-hand-side quantity of Eq. (18),  $\tilde{\eta}^2/\eta_\sigma^2$ , describes the enhancement of the estimate precision, in terms of the signal-to-noise ratio. However, from Eq. (13), we find that the precision enhancement factor is given by  $\eta/\eta_\sigma$ , with  $\eta$  (but not  $\tilde{\eta}$ ) the signal amplification rate. If we alternatively use  $\eta$  to replace  $\tilde{\eta}$  in the inequality (18), we have found (numerically) that the inequality (18) cannot be valid in general. It can be violated for some measurement strength and post-selection. This indicates that, strictly speaking, the Fisher information characterization is not precisely equivalent to the characterization of the signal-to-noise ratio, say, Eq. (13).

## IV. EFFECT OF TECHNICAL NOISE

In the previous analysis of the SNR, the ‘noise’ is actually the quantum uncertainty of quantum measurement. In real experiments, there exist other possible technical issues. In this work we will follow the noise model of Knee and Gauger [28], which might represent the transverse beam-displacement jitter in the quantum optical setup and can properly account for the amplifier’s noise in the quadrature measurements of the microwave photons in the circuit QED experiments. Similar models have also been considered in Refs. [8, 15, 26, 27].

### A. Measurement in the $x$ basis: $x_0$ noise

Let us first consider the technical noise  $x_0$ , which shifts the meter’s wavefunction, e.g., associated with the initial state  $|i\rangle$ , from  $P_i(x)$  to  $P_i(x - x_0)$ , while the noise is assumed to be

the typical Gaussian

$$\Pr(x_0) = \frac{1}{\sqrt{2\pi}J} e^{-x_0^2/2J^2}, \quad (19)$$

where  $J$  is the width of the noise distribution. Straightforwardly, the *joint probability* of getting  $x$  under the initial state  $|i\rangle$  and passing the postselection of  $|f\rangle$ , and as well with the specific noise  $x_0$ , is given by

$$\Pr(f; x, x_0) = P_i(x - x_0) P_{x-x_0}(f) \Pr(x_0)/\mathcal{N}_f, \quad (20)$$

where  $\mathcal{N}_f$  is a normalization factor (given by integrating the variables  $x$  and  $x_0$ ). The two probabilities involved in this result simply read  $P_i(y) = \sum_{j=1,2} \rho_{ijj} P_j(y)$  and  $P_y(f) = \langle f|\tilde{\rho}(y)|f\rangle$ , with a substitution of  $y = x - x_0$ . Then, we can carry out any averages under the joint probability through  $f\langle\bullet\rangle_i = \int dx_0 \int dx \langle\bullet\rangle \Pr(f; x, x_0)$ . In particular, the two quantities of our interest are obtained as

$$\begin{aligned} f\langle x\rangle_i &= \left(\frac{\text{Re}A_w}{\mathcal{M}}\right) d, \\ f\langle x^2\rangle_i &= \sigma^2 + J^2 + \left(\frac{\eta d^2}{2}\right) \left(\frac{1+|A_w|^2}{\text{Re}A_w}\right). \end{aligned} \quad (21)$$

We find that the shift of the signal is not affected by the noise. However, as expected, the variance of the amplified signal is added by  $J^2$ , by noting that  $f\langle x^2\rangle_i - (f\langle x\rangle_i)^2 = \tilde{\sigma}^2 + J^2$  and  $\tilde{\sigma}^2$  is the result shown in Eq.(11), i.e., the variance in the absence of noise. These two features are the same as in the AAV limit, despite that the variance  $\tilde{\sigma}^2$  depends on the measurement strength.

## B. Measurement in the $p$ basis: $x_0$ noise

Following Ref. [26], we consider next the more interesting scheme of the so-called *imaginary* WVA technique, which involves the weak measurement in the  $p$  basis, i.e., the eigenbasis of the coupling operator  $P$  in the interaction Hamiltonian  $H' = \kappa PA$ . The basic idea is as follows. We know that the unitary evolution, under the action of  $U = e^{-idPA}$ , would result in the entangled state of Eq.(1). Our previous analysis is based on the measurement in the  $x$ -basis, which makes us express the wavefunction of the meter's states as  $\Phi_{1,2}(x) = (2\pi\sigma^2)^{-1/4} \exp[-(x \mp d)^2/4\sigma^2]$ . Now, since we are interested in measurement in the  $p$ -basis, after a simple Fourier transformation, the meter's wavefunctions read  $\Phi_{1,2}(p) = (\frac{\pi}{2}\sigma^{-2})^{-1/4} \exp[-\sigma^2 p^2 \mp idp]$ . As we will see shortly, the postselection-associated weak measurement in the  $p$ -basis will result in a weak-value-amplification proportional to  $\text{Im}A_w$ , i.e., the imaginary part of the AAV weak value, which is thus called *imaginary* WVA technique.

Further, if the noise is introduced as well by  $x_0$ , i.e., a random shift of the meter's wavefunction in the  $x$  basis, the meter's wavefunctions in the  $p$  basis can be reexpressed as

$$\Phi_{1,2}(p; x_0) = \left(\frac{\pi}{2}\sigma^{-2}\right)^{-1/4} \exp[-\sigma^2 p^2 \mp idp - ix_0 p] \quad (22)$$

Associated with these two wavefunctions, one can check that the Bayesian approach for state inference does not work.

However, one can update the system state based on the meter's result of  $p$  from the elements of the density matrix  $\rho_T = |\Psi_T\rangle\langle\Psi_T|$ , say, from  $\rho_{jk}(p) = \langle j|p\rangle\langle\rho_T|p\rangle\langle k|$  (with  $j, k = 1$  and  $2$ ). More explicitly, the system state conditioned on the result  $p$  is simply given by

$$\tilde{\rho}_{jk}(p) = \rho_{ijk} \Phi_j(p, x_0) \Phi_k^*(p, x_0) / \mathcal{N}(p, x_0), \quad (23)$$

where the normalization factor reads  $\mathcal{N}(p, x_0) = \sum_{j=1,2} \rho_{ijj} |\Phi_j(p, x_0)|^2$ . We can easily check that the diagonal elements of the system state remain unchanged under the  $p$  basis measurement, while the off-diagonal elements are updated, for instance, as

$$\tilde{\rho}_{12}(p) = \rho_{112} e^{-i2dp}. \quad (24)$$

Then, the joint probability reads

$$\Pr(f; p, x_0) = P_i(p, x_0) P_p(f) \Pr(x_0)/\mathcal{N}_f, \quad (25)$$

with  $P_i(p, x_0) = \mathcal{N}(p, x_0)$ ,  $P_p(f) = \langle f|\tilde{\rho}(p)|f\rangle$ , and  $\mathcal{N}_f$  a normalization factor. We find that the both probabilities are free from the noise  $x_0$ , knowing thus that any averages of  $p$ 's functions are free from  $x_0$ . Then, an important conclusion is that based on this measurement scheme, the WVA technique for parameter estimation can eliminate the negative effect of this type of noise. Actually, our present result generalizes this claim from the AAV limit to finite strength of measurement.

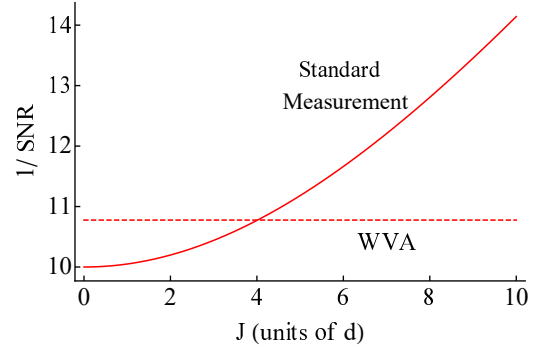


FIG. 5: Inverse plot of the SNR, for a clearer comparison of  $R_{S/N}^{(w)}$  (imaginary WVA measurement) with  $R_{S/N}^{(s)} = d/\sqrt{\sigma^2 + J^2}$  (standard measurement), while the latter contains the broadening width  $J^2$  from the  $x_0$  noise, unlike  $R_{S/N}^{(w)}$  which is free from the noise. The PPS states are chosen as  $|i\rangle = (|1\rangle + |2\rangle)/\sqrt{2}$  and  $|f\rangle = \cos\frac{\theta}{2}e^{i\varphi}|1\rangle + \sin\frac{\theta}{2}|2\rangle$ , with  $\theta = 1.49\pi$  and  $\varphi = \pi/4$ . The measurement strength in this plot is associated with a choice of  $d = 1$  and  $\sigma = 10$  (in a system of arbitrary units).

Using the joint probability  $\Pr(f; p, x_0)$ , the postselection conditioned averages of  $p$  and  $p^2$  can be easily obtained

$$\begin{aligned} f\langle p\rangle_i &= \left(\frac{\text{Im}A_w}{\mathcal{M}}\right) \left(\frac{d}{2\sigma^2}\right) e^{-d^2/2\sigma^2}, \\ f\langle p^2\rangle_i &= \frac{1}{4\sigma^2} + \left(\frac{|A_w|^2 - 1}{\mathcal{M}}\right) \left(\frac{d^2}{8\sigma^4}\right) e^{-d^2/2\sigma^2}. \end{aligned} \quad (26)$$

Notice that the first result, say, the new *signal*, cannot be regarded as an amplification of the old signal  $d$ , owing to the

measurement performed in a different basis. One can easily check that, for the  $p$  basis measurement and without postselection, the ‘signal’ is zero. Therefore, in this case, the proper characterization is the direct use of the SNR in the  $p$  basis measurement

$$R_{S/N}^{(w)} = \frac{\sqrt{\gamma} f\langle p \rangle_i}{[\delta_w^2(p)]^{1/2}}, \quad (27)$$

where the variance of the postselected result is given by  $\delta_w^2(p) = f\langle p^2 \rangle_i - (f\langle p \rangle_i)^2$ . In Fig. 5, we make a numerical comparison between  $R_{S/N}^{(w)}$  and  $R_{S/N}^{(s)}$ , while the latter is the SNR of the standard measurement,  $R_{S/N}^{(s)} = d/\sqrt{\sigma^2 + J^2}$ , which contains the broadening  $J^2$  from the  $x_0$  noise, unlike  $R_{S/N}^{(w)}$  which is free from the noise. We find that the imaginary-WVA technique outperforms the standard method when the noise exceeds certain modest strength, while both schemes have similar SNR in the absence of noise.

### C. Measurement in the $p$ basis: $p_0$ noise

Let us continue to consider the measurement in the  $p$  basis, but now with a noise caused by a random  $p_0$  shift of the  $p$  wavepacket. The noise is assumed as well a Gaussian

$$\Pr(p_0) = \frac{1}{\sqrt{2\pi}J_p} e^{-p_0^2/2J_p^2}, \quad (28)$$

with  $J_p$  the width of the noise distribution. For a specific  $p_0$ , the meter’s wavefunctions are shifted from  $\Phi_{1,2}(p)$  to  $\Phi_{1,2}(p - p_0) = (\frac{\pi}{2}\sigma^{-2})^{-1/4} \exp[-\sigma^2(p - p_0)^2 \mp idp]$ . Then, conditioned on the  $p$  result of the measurement, the state can be easily updated as  $\tilde{\rho}_{12}(p) = \rho_{i12} e^{-i2dp}$ , while the diagonal elements of the density matrix remain unchanged.

Similarly as above, the joint probability in this case reads

$$\Pr(f; p, p_0) = P_i(p, p_0) P_p(f) \Pr(p_0) / \mathcal{N}_f, \quad (29)$$

where the initial-state-related probability of getting  $p$  is given by  $P_i(p, p_0) = \sum_{j=1,2} \rho_{ijj} |\Phi_j(p - p_0)|^2$ , the postselection probability is given by  $P_p(f) = \langle f | \tilde{\rho}(p) | f \rangle$ , and the normalization factor  $\mathcal{N}_f$  is given by integrating the variables  $p$  and  $p_0$ . Accordingly, the postselection conditioned average can be done through  $f\langle \bullet \rangle_i = \int dp_0 \int dp \langle \bullet \rangle \Pr(f; p, p_0)$ , which yields

$$f\langle p \rangle_i = \left( \frac{\text{Im}A_w}{\mathcal{M}_k} \right) (2d/\tilde{\sigma}_J^2) e^{-2d^2/\tilde{\sigma}_J^2}, \\ f\langle p^2 \rangle_i = 1/\tilde{\sigma}_J^2 + \left( \frac{|A_w|^2 - 1}{\mathcal{M}_k} \right) (2d^2/\tilde{\sigma}_J^4) e^{-2d^2/\tilde{\sigma}_J^2}. \quad (30)$$

Here we introduced the second *modification* factor beyond the AAV limit,  $\mathcal{M}_k = 1 + K(|A_w|^2 - 1)$ , with the measurement strength related factor  $K$  given by  $K = (1 - e^{-2d^2/\tilde{\sigma}_J^2})/2$ . We also introduced an *effective width* of uncertainty through

$$1/\tilde{\sigma}_J^2 = \frac{1}{4\sigma^2} + J_p^2. \quad (31)$$

As above, the first result in Eq. (30) cannot be understood as an amplification of the original signal  $d$ . Also, the reasonable characterization in this case is again using the SNR defined by Eq. (27).

In Fig. 6, we numerically show the effect of the  $p_0$  noise on the SNR. We may first check that, in the absence of the  $p_0$  noise, for the quantum widths  $\sigma = (10, 20, 100)$ , the corresponding SNRs based on the imaginary WVA measurement,  $R_{S/N}^{(w)} = (0.093, 0.046, 0.009)$ , are comparable to that from the standard method, i.e.,  $R_{S/N}^{(s)} = (0.1, 0.05, 0.01)$ . Then, after introducing the  $p_0$  noise, very strikingly, we find that one can even use the noise to increase the estimate precision, with the increase of  $J_p$  until a critical value  $J_p^*$ . From Fig. 6, taking  $\sigma = 100$  as an example, the SNR is enhanced by the noise by a factor of  $\mathcal{R} \simeq 0.45/0.01 = 45$ . This is indeed a remarkable result, in regard to the practical use of the imaginary WVA technique [26].

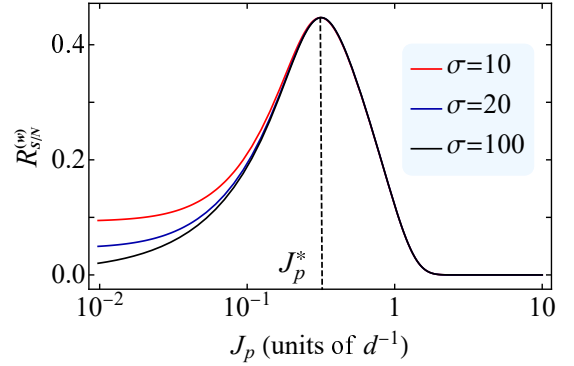


FIG. 6: Effect of the  $p_0$  noise on the SNR of the imaginary WVA measurement. In the absence of the  $p_0$  noise, the SNR is comparable to that of the standard method. Very strikingly, however, after introducing the  $p_0$  noise, the result shows that one can use the noise to enhance the estimate precision, with the increase of the noise width  $J_p$  until a critical value  $J_p^*$ . The same PPS states are chosen as in Fig. 5 and the measurement strengths are associated with the choice of  $d = 1$  and a few  $\sigma$  as shown in the figure (in a system of arbitrary units).

The critical value of the noise strength, i.e.,  $J_p^*$  shown in Fig. 6, is determined by the interplay of the a few factors in the signal-to-noise ratio expression, Eq. (27). First, consider the postselected average  $f\langle p \rangle_i$ . It has a turnover behavior, qualitatively like that observed in Fig. 5. Indeed, this turnover behavior is dominantly caused by the two factors,  $2d/\tilde{\sigma}_J^2$  and  $e^{-2d^2/\tilde{\sigma}_J^2}$ , in Eq. (30). However, after a careful check, the modification factor  $\mathcal{M}_k$  in  $f\langle p \rangle_i$  influences also the location of the peak. Another more prominent influence on the location of the peak is from the denominator  $[\delta_w^2(p)]^{1/2}$  in the signal-to-noise ratio, which is a monotonically increasing function with  $J_p$  and shifts the peak to a smaller value of  $J_p^*$ . Finally, the post-selection probability  $\gamma$ , which slowly increases with  $J_p$ , also has an observable influence on the location of the peak.

We notice that, based on the treatment under the AAV assumptions, the analytic solution derived in Ref. [26] cannot



predict the turnover behavior as shown in Fig. 5. Under the AAV limit, the SNR was found to be enhanced monotonically by the noise strength  $J_p$ . In Ref. [26], the validity condition of the AAV *effect* has been carefully argued, which is needed to ensure the derived expression of the SNR to be valid. In order to eliminate the unreasonable prediction at large  $J_p$ , numerical results beyond the AAV limit were displayed in Ref. [26] as a necessary correction. In this context, we may mention that our treatment and the obtained analytic result Eq. (30) make the SNR be valid (with the turnover behavior) without any further modifications. Finally, we may also mention that the turnover behavior and the important enhancement of the SNR are an overall consequence of the type of the interaction Hamiltonian (with the  $P$  operator), the  $p$ -basis measurement, the postselection, and the type of the technical noise introduced in the imaginary WV measurement. The results are not obvious from a simple intuition, but nontrivially involve certain complexity of mathematics.

## V. SUMMARY

We have presented a generalization study for the WVA technique of parameter estimation, in terms of characterizations of SNR and Fisher information. Our generalizations were based on the quantum Bayesian approach (or its variant) for partial-collapse weak measurement with arbitrary strength. By constructing the joint probability distribution function associated with postselection and the possible techni-

cal noise, we were able to carry out the various analytical expressions for the expectation and variance of the postselected measurement results of the meter's variable. We thus obtained analytic results of the SNR and presented systematic analysis in combination with numerical illustration.

A couple of interesting conclusions may be drawn from our generalized results, such as that in practice one should avoid too 'anomalously' large AAV WV (in contrast to the naive expectation based on the AAV's treatment), and can design technical noise strength to achieve optimal SNR in the imaginary WVA measurement, as well as that the Fisher information characterization is not fully equivalent to the SNR characterization with the increase of measurement strength. We expect that these conclusions can attract attentions of the WVA community, from either the experimental perspective or a purely theoretical interest. We also expect the treatment method to be applied in the various experimental explorations.

*Acknowledgements.*— This work was supported by the National Key Research and Development Program of China (No. 2017YFA0303304) and the NNSF of China (Nos. 11675016, 11974011 & 61905174).

- 
- [1] Y. Aharonov, D. Z. Albert, and L. Vaidman, *How the result of a measurement of a component of the spin of a spin-1/2 particle can turn out to be 100*, Phys. Rev. Lett. **60**, 1351 (1988).
  - [2] Y. Aharonov and L. Vaidman, *Properties of a quantum system during the time interval between two measurements*, Phys. Rev. A **41**, 11 (1990).
  - [3] J. S. Lundeen, B. Sutherland, A. Patel, C. Stewart, and C. Bamber, *Direct measurement of the quantum wavefunction*, Nature **474**, 188 (2011).
  - [4] J. Z. Salvail, M. Agnew, A. S. Johnson, E. Bolduc, J. Leach, and R. W. Boyd, *Full characterisation of polarisation states of light via direct measurement*, Nat. Photon. **7**, 316 (2013).
  - [5] M. Malik, M. Mirhosseini, M. P. J. Lavery, J. Leach, M. J. Padgett, and R. W. Boyd, *Direct measurement of a 27-dimensional orbital-angular-momentum state vector*, Nat. Commun. **5**, 3115 (2014).
  - [6] O. Hosten and P. G. Kwiat, *Observation of the Spin Hall Effect of Light via weak measurements*, Science **319**, 787 (2008).
  - [7] P. B. Dixon, D. J. Starling, A. N. Jordan, and J. C. Howell, *Ultrasensitive beam deflection measurement via interferometric weak value amplification*, Phys. Rev. Lett. **102**, 173601 (2009).
  - [8] D. J. Starling, P. B. Dixon, A. N. Jordan, and J. C. Howell, *Optimizing the signal-to-noise ratio of a beam-deflection measurement with interferometric weak values*, Phys. Rev. A **80**, 041803 (2009).
  - [9] D. J. Starling, P. B. Dixon, N. S. Williams, A. N. Jordan, and J. C. Howell, *Continuous phase amplification with a sagnac interferometer*, Phys. Rev. A **82**, 011802 (2010).
  - [10] D. J. Starling, P. B. Dixon, A. N. Jordan, and J. C. Howell, *Precision frequency measurements with interferometric weak values*, Phys. Rev. A **82**, 063822 (2010).
  - [11] G. I. Viza, J. Martínez-Rincón, G. A. Howland, H. Frostig, I. Shomroni, B. Dayan, and J. C. Howell, *weak-values technique for velocity measurements*, Opt. Lett. **38**, 2949 (2013).
  - [12] N. Brunner and C. Simon, *Measuring small longitudinal phase shifts: weak measurements or standard interferometry?*, Phys. Rev. Lett. **105**, 010405 (2010).
  - [13] J. M. Hogan, J. Hammer, S. W. Chiow, S. Dickerson, D. M. S. Johnson, T. Kovachy, A. Sugarbaker, and M. A. Kasevich, *Precision angle sensor using an optical lever inside a sagnac interferometer*, Opt. Lett. **36**, 1698 (2011).
  - [14] M. D. Turner, C. A. Hagedorn, S. Schlamminger, and J. H. Gundlach, *Picoradian deflection measurement with an interferometric quasi-autocollimator using weak value amplification*, Opt. Lett. **36**, 1479 (2011).
  - [15] A. Feizpour, X. Xingxing, and A. M. Steinberg, *Amplifying single-photon nonlinearity using weak measurements*, Phys. Rev. Lett. **107**, 133603 (2011).
  - [16] X. Y. Xu, Y. Kedem, K. Sun, L. Vaidman, C. F. Li, and G. C. Guo, *Phase estimation with weak measurement using a white light source*, Phys. Rev. Lett. **111**, 033604 (2013).
  - [17] G. I. Viza, J. Martínez-Rincón, W. T. Liu, and J. C. Howell, *Complementary weak-value amplification with concatenated postselections*, Phys. Rev. A **94**, 043825 (2016).
  - [18] J. Martínez-Rincón, C. A. Mullarkey, G. I. Viza, W. T. Liu, and J. C. Howell, *Ultra sensitive inverse weak-value tilt meter*, Opt.

- Lett. **42**, 2479 (2017).
- [19] S. Pang, J. R. G. Alonso, T. A. Brun, and A. N. Jordan, *Protecting weak measurements against systematic errors*, Phys. Rev. A **94**, 012329 (2016).
- [20] J. Sinclair, M. Hallaji, A. M. Steinberg, J. Tollaksen, and A. N. Jordan, *Weak-value amplification and optimal parameter estimation in the presence of correlated noise*, Phys. Rev. A **96**, 052128 (2017).
- [21] J. Harris, R. W. Boyd, and J. S. Lundeen, *Weak value amplification can outperform conventional measurement in the presence of detector saturation*, Phys. Rev. Lett. **118**, 070802 (2017).
- [22] X. Qiu, L. Xie, X. Liu, L. Luo, Z. Zhang, and J. Du, *Estimation of optical rotation of chiral molecules with weak measurements*, Opt. Lett. **41**, 4032 (2016).
- [23] D. Li, Z. Shen, Y. He, Y. Zhang, Z. Chen, and H. Ma, *Application of quantum weak measurement for glucose concentration detection*, Appl. Opt. **55**, 1697 (2016).
- [24] A. K. Singh, S. K. Ray, S. Chandel, S. Pal, A. Gupta, P. Mitra, and N. Ghosh, *Tunable Fano resonance using weak-value amplification with asymmetric spectral response as a natural pointer*, Phys. Rev. A **97**, 053801(2018).
- [25] A. Nishizawa, K. Nakamura, and M. K. Fujimoto, *Weak value amplification in a shot-noise-limited interferometer*, Phys. Rev. A **85**, 062108 (2012).
- [26] Y. Kedem, *Using technical noise to increase the signal-to-noise ratio of measurements via imaginary weak values*, Phys. Rev. A **85**, 060102(R) (2012).
- [27] A. N. Jordan, J. Martinez-Rincon, and J. C. Howell, *Technical advantages for weak-value amplification: when less is more*, Phys. Rev. X **4**, 011031 (2014).
- [28] G. C. Knee and E. M. Gauger, *When amplification with weak values fails to suppress technical noise*, Phys. Rev. X **4**, 011032 (2014).
- [29] S. Tanaka and N. Yamamoto, *Information amplification via postselection: a parameter-estimation perspective*, Phys. Rev. A **88**, 042116 (2013).
- [30] C. Ferrie and J. Combes, *Weak value amplification is suboptimal for estimation and detection*, Phys. Rev. Lett. **112**, 040406 (2014).
- [31] N. S. Williams and A. N. Jordan, *Weak values and the Leggett-Garg inequality in solid-state qubits*, Phys. Rev. Lett. **100**, 026804 (2008).
- [32] A. Di Lorenzo and J. C. Egues, *Weak measurement: effect of the detector dynamics*, Phys. Rev. A **77**, 042108 (2008).
- [33] X. Zhu, Y. Zhang, S. Pang, C. Qiao, Q. Liu, and S. Wu, *Quantum measurements with preselection and postselection*, Phys. Rev. A **84**, 052111 (2011).
- [34] T. Koike and S. Tanaka, *Limits on amplification by Aharonov-Albert-Vaidman weak measurement*, Phys. Rev. A **84**, 062106 (2011).
- [35] K. Nakamura, A. Nishizawa, and M. K. Fujimoto, *Evaluation of weak measurements to all orders*, Phys. Rev. A **85**, 012113 (2012).
- [36] Y. Susa, Y. Shikano, and A. Hosoya, *Optimal probe wave function of weak-value amplification*, Phys. Rev. A **85**, 052110 (2012).
- [37] A. G. Kofman, S. Ashhab, and F. Nori, *Nonperturbative theory of weak pre- and post-selected measurements*, Phys. Rep. **520**, 43 (2012).
- [38] L. Qin, P. Liang, and X. Q. Li, *Weak values in continuous weak measurement of qubits*, Phys. Rev. A **92**, 012119 (2015).
- [39] L. Qin, W. Feng, and X. Q. Li, *Simple understanding of Quantum weak values*, Scientific Reports **6**, 20286 (2016).
- [40] L. Qin, L. Xu, W. Feng, and X. Q. Li, *Qubit state tomography in superconducting circuit via weak measurements*, New J. Phys. **19**, 033036 (2017).
- [41] A. N. Korotkov, *Continuous quantum measurement of a double dot*, Phys. Rev. B **60**, 5737 (1999).
- [42] A. N. Korotkov, *Quantum Bayesian approach to circuit QED measurement*, arXiv:1111.4016.
- [43] P. Wang, L. Qin, and X. Q. Li, *Quantum Bayesian rule for weak measurements of qubits in superconducting circuit QED*, New J. Phys. **16**, 123047 (2014); *ibid*, New J. Phys. **17**, 059501 (2015).
- [44] W. Feng, P. Liang, L. Qin, and X. Q. Li, *Exact quantum Bayesian rule for qubit measurements in circuit QED*, Scientific Reports **6**, 20492 (2016).
- [45] H. M. Wiseman and G. J. Milburn, *Quantum Measurement and Control* (Cambridge Univ. Press, Cambridge, 2009).